# Impact of Regioregularity on Alignment and Thermoelectric Properties of Sequentially Doped and Oriented Films of Poly(3-hexylthiophene)

Shubhradip Guchait, Laurent Herrmann, Karim Kadri, Nicolas Leclerc, François Tran-Van, Martin Brinkmann

# Impact of regioregularity on alignment and thermoelectric properties of sequentially doped and oriented films of poly(3-hexylthiophene)

Shubhradip Guchait [1], Laurent Herrmann [1], Karim Kadri [2], Nicolas Leclerc [3], François Tran Van [2], Martin Brinkmann [1]*

(1) *Université de Strasbourg, CNRS, ICS UPR 22, F-67000 Strasbourg, France,*

*(2) Laboratoire de Physico-Chimie des Matériaux et des Electrolytes pour l'Energie (PCM2E), EA6299, Université de Tours, 37200 Tours, France*

(3) Université de Strasbourg, CNRS, ICPEES UMR 7515, F-67087 Strasbourg, France

* e-mail : martin.brinkmann@ics-cnrs.unistra.fr

## Abstract

Alignment of conjugated polymers such as regioregular poly(3-hexylthiophene-2,5-diyl) (rr-P3HT) is an effective means to enhance charge transport and thermoelectric properties of thin films doped with $F_4TCNQ$. In this contribution, we investigate the impact of P3HT regioregularity (RR) on the alignment achieved in thin films by high temperature rubbing and the resulting thermoelectric properties in sequentially doped and aligned films. Structure and thermoelectric properties in doped P3HT thin films are investigated by a combination of transmission electron microscopy (electron diffraction), polarized UV-vis-NIR spectroscopy and thermoelectric measurements. Despite limited thermomechanical properties, rubbing at 165°C generates order and alignment in 71%RR P3HT (R71-P3HT) with a typical lamellar stacking of P3HT chains similar to that of the smectic-like phase of RR-P3HT. Order is further enhanced in aligned R71-P3HT films by doping with $F_4TCNQ$. Intercalation of dopants in the ordered domains of R71-P3HT induces a reorganization of polythiophene backbones within individual π-stacks with lattice parameter variations equivalent to those observed for RR-P3HT. Despite ordering induced by both rubbing at 165°C and doping, charge conductivity of oriented R71-P3HT in the chain direction remains 50-times below that of oriented RR-P3HT. The strong blue-shift of the polaronic bands in R71-P3HT versus RR-P3HT indicates that polarons are strongly localized in both ordered and amorphous zones of R71-P3HT, explaining the modest charge conductivity of 3-4 S/cm observed in the chain direction.

Keywords: conducting polymers, thermoelectricity, conjugated polymers, crystallization, transmission electron microscopy

## I.Introduction.

In the last decade, doped polymer semiconductors (PSCs) emerged as key materials for potential applications in organic thermoelectrics.[1] Remarkable progress has been made on the performances of such organic thermoelectric (TE) materials, especially for p-type systems.[2,3] Central for the optimization of TE properties in doped PSCs is the control over material processing including PSC crystallization/alignment and doping.[4] Doping is key as it is a classical means to tune the density of charge carriers in the PSCs. Redox doping of p-type PSCs with strong electron acceptor molecules such as 2,3,5,6-tetrachlorofluoro-7,7,8,8-tetracyanoquinodimethane ($F_4$TCNQ) has been widely used to transform semiconducting polymers such as regioregular poly(3-hexylthiophene) (RR-P3HT) into conducting polymers with interesting TE properties.[5] P3HT/$F_4$TCNQ is a model system that has been intensively investigated to uncover the correlations between charge transport, structure and processing.[5-9] Doping PSCs can be performed either in solution by mixing directly the polymer and the dopant in a common solvent, or by so-called sequential doping whereby the crystallization and alignment of the PSC film can be separated from the doping step.[7] Such sequential doping either from solution or using the vapor phase of the dopants results often in superior TE properties than co-processing of polymer and dopant.[10] As demonstrated by various groups, the crystalline structure of the pristine PSC has a strong impact on the resulting TE properties, higher crystallinity leads to improved charge conductivity and TE properties.[11,12,13] Besides crystallinity, orientation of PSCs also proved beneficial to enhance the thermoelectric figure of merit and power factor of the doped RR-P3HT films.[14-16] Alignment of the PSCs enhances both charge conductivity and the Seebeck coefficient in the chain direction.[13,15,17,18]

In P3HT, the crystallinity is largely determined by the regioregularity of the polymer. Regio-random P3HT (RRa-P3HT, Figure 1.a) is essentially amorphous contrary to RR-P3HT, leading to very poor charge transport properties in doped films.[12,19] Usually, the crystallinity of P3HT increases with regioregularity, typically from 18% for RR=75%. to 48% for RR=96% [19,20] However, several groups reported that regiorandom P3HT shows ordering upon doping thin films with $F_4TCNQ$.[20,21] Characteristic reflections of ordered RR-P3HT such as 1 0 0 (lamellar periodicity) and 0 2 0 (π-stacking distance) appear after doping RRa-P3HT with $F_4TCNQ$.[22,23] In addition, it has been demonstrated that the TE power factor of RR-P3HT can be enhanced in the chain direction in thin films that were oriented by high-T rubbing.[13] When oriented RR-P3HT is doped with either magic blue or Mo(tdf-$COCF_3)_3$, very high thermoelectric power factors of 160 $\mu W \cdot m^{-1} \cdot K^{-2}$ were obtained.[24,25] The advantage of working with oriented PSC films relates also to the possibility to differentiate the doping of crystalline and amorphous zones of the polymer using polarized UV-vis-NIR spectroscopy.[13,25] Moreover, recent studies on electrochemical doping of poorly ordered RR-P3HT films demonstrated that high charge conductivities beyond 200 S/cm can be reached despite poor crystallinity.[26] It seems therefore interesting to combine alignment of RRa-P3HT and sequential doping (using for instance incremental concentration doping) to better understand how doping occurs in regiorandom P3HT and how it differs from RR-P3HT (Figure 1.a and 1.b). The impact of P3HT regioregularity on the alignment achieved by high-T rubbing has so far never been investigated and is accordingly the focus of the first part of this contribution. We investigate how the temperature of rubbing affects structure and orientation of P3HT with RR=71% (R71-P3HT) and compare it to P3HT with RR≥96% (RR-P3HT). In the second part of this work, we evaluate how doping modifies the structure of aligned R71-P3HT films and what are the resulting charge transport and TE properties. Notably, we show that both high-T rubbing and doping are able to induce ordering of R71-P3HT. The doping mechanism of R71-

P3HT is similar to that observed for the smectic-like phase of RR-P3HT with the intercalation of $F_4TCNQ$ dopant molecules in the side chain layers of R71-P3HT with their long axis in plane perpendicular to the P3HT chains. The final TE properties of aligned and doped R71-P3HT are anisotropic and approach those of non-oriented RR-P3HT.

**II.Results.**

**1) Impact of regioregularity on the orientation and structure of P3HT films aligned by high-T rubbing.**

As demonstrated in previous studies, the rubbing temperature $T_R$ is the most important parameter controlling the orientation and structure of rubbed RR-P3HT films. For RR-P3HT, rubbing at $T_R$ around 100°C produces aligned films with a smectic-like structure whereas for $150°C \leq T_R \leq 240°C$, semi-crystalline P3HT films with a periodic lamellar structure are obtained. (27,28) The alignment of RR-P3HT improves substantially for $T_R \geq 100°C$ and the dichroic ratio $DR=A_{//}/A_{\perp}$ can reach values of 12-15 for $T_R \geq 180°C$ corresponding to 3D order parameters ($OP=(DR-1)/(DR+2)$) up to 0.85.[26] Moreover, the vibronic structure of the spectrum in aligned RR-P3HT for POL//R shows an increase of the 0-0 component over 0-1 with increasing $T_R$ that relates to a progressive reduction in the excitonic bandwidth W with $T_R$ (see Figure 1.c).

To probe the impact of regioregularity on orientation of P3HT by high-T rubbing, we used a P3HT sample with a regioregularity of 71% obtained by electrochemical synthesis (see experimental section). Let us see now how R71-P3HT behaves upon rubbing. Figure 1.e depicts the evolution of the DR for R71-P3HT films rubbed at various $T_R$. The alignment of R71-P3HT is very different from that of RR-P3HT. First, the alignment remains very modest and a maximum OP = 0.44 (DR in the range 3-4) is obtained for $T_R$=165°C (Figure 1.e). For

$T_R \geq 170°C$ the film is mechanically damaged with a strong delamination from the substrate. This is consistent with the fact that P3HT with a regioregularity of 75% shows an onset of melting around 170°C.[20,21] The evolution of the normalized UV-vis spectrum of rubbed R71-P3HT for POL//R shows that by increasing the rubbing temperature, the 0-0 and 0-1 components of the vibronic structure of P3HT become more intense (Figure 1.f). Interestingly, films of R71-P3HT prepared by doctor blading at 150°C from a solution in *o*DCB show almost no vibronic structure and the absorption spectrum is peaked around 500nm, which is typical for amorphous P3HT films. Accordingly, high-T rubbing is able to enforce order in R71-P3HT especially for $T_R$ close to 165°C. The spectrum for POL⊥R further indicates that a part of the rubbed R71-P3HT films remains amorphous as indicated by the unstructured and 500nm-peaked absorption. Accordingly, for $T_R$=165°C, rubbed R71-P3HT films consist of a coexistence of ordered and fully amorphous domains.

Polarized UV-vis spectroscopy helps further evaluate the level of order in the R71-P3HT films from the vibronic structure of the UV-vis absorption band.[29,30] The ratio of absorbances of the 0-0 and 0-1 helps extract the so-called excitonic band width W that is a measure of crystalline order in P3HT thin films.[30] Moreover, it has been shown that W is correlated to the charge transport: the lower W, the higher the charge mobility in P3HT.[29] For the best oriented and ordered R71-P3HT films W=70 meV *versus* 39 meV for RR-P3HT films rubbed at 200°C. Accordingly, and consistently with TEM studies (vide infra), order in aligned R71-P3HT remains well below that found for the best oriented semi-crystalline RR-P3HT ($T_R$=180°C). The vibronic structure seen in R71-P3HT films aligned at 165°C is comparable to that of RR-P3HT films rubbed at 100°C that have a smectic-like structure i.e. a layered structure made of i) π-stacks of polythiophene backbones without translational order (i.e. registry) of thiophenes in the chain direction within the stacks and ii) layers of disordered side chains. [27,28] Accordingly, polarized UV-vis spectroscopy demonstrates that rubbing R71-

P3HT films at 165°C produces aligned films with enhanced crystalline order similar to the smectic-like phase of RR-P3HT.

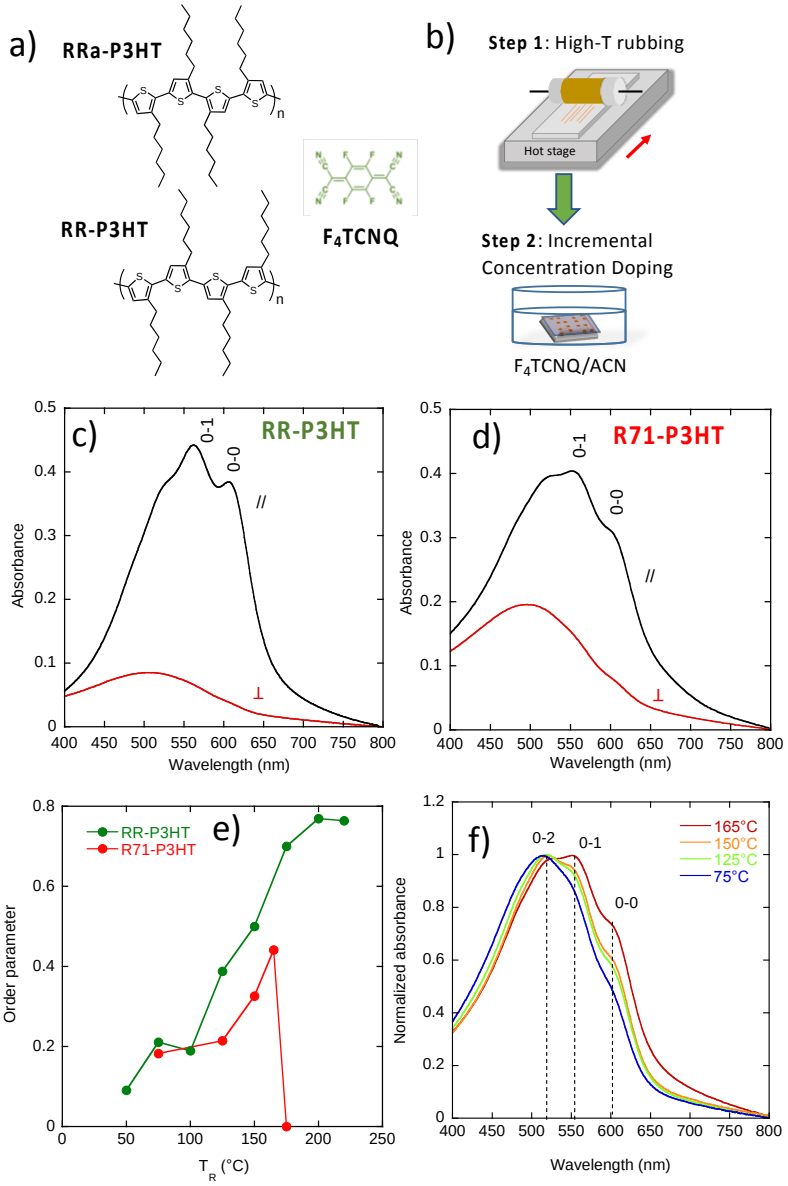


***Figure 1***. *a) Molecular structures of Regio-Random P3HT (R71-P3HT) and Regio-Regular P3HT (RR-P3HT), $F_4TCNQ$ dopant. b) Preparation of conducting and oriented PSC films by a combination of high-T rubbing and sequential doping. c) and d) Polarized UV-vis-NIR spectra of RR-P3HT and R71-P3HT corresponding to optimal alignment conditions (200°C for RR-P3HT and 165°C for R71-P3HT). e) Evolution of the order parameter OP=(DR-1)/(DR+2) calculated from the dichroic ratio DR for the 0-0 absorption band as a function of rubbing temperature $T_R$ for R71-P3HT and RR-P3HT f) Evolution of the vibronic structure in*

*thin films of R71-P3HT for i) the pristine film (doctor bladed at 150°C in ODCB) and ii) films oriented by high-T rubbing at increasing temperatures $T_R$.*

Regarding the structure of the oriented R71-P3HT, it was analyzed using electron diffraction. The evolution of the ED patterns with $T_R$ is shown in Figure S1. Clearly, for $T_R$=125°C, the ED patterns show a quasi-continuous Scherrer ring corresponding to the 0 2 0 reflection (π-stacking) with some intensity accentuations on the equator. This reflection coexists with a very weak equatorial 1 0 0. This indicates that for $T_R$=125°C, the rubbed R71-P3HT films consist of a majority of edge-on crystals with random in-plane orientation and a minority of aligned face-on R71-P3HT domains.

A marked change in the ED is observed for $T_R \geq 150$°C. For $T_R$=165°C, the ED shows intense equatorial h 0 0 (h=1-3) and 0 2 0 reflections. Accordingly, for $T_R$=165°C, the R71-P3HT films consist of a mixture of in-plane oriented edge-on and face-on ordered domains. Although multiple orders of the lamellar periodicity are seen, the ED pattern of oriented R71-P3HT films remains poor without multiple index reflections. This is a consequence of the regio-random branching of the side chains that is responsible for the absence of the 0 0 2 reflection in the ED pattern, it is similar to that of the smectic-like phase of rubbed P3HT i.e. without registry of stacking of thiophene units inside individual π-stacks.[28] This is fully consistent with the results of polarized UV-vis-NIR spectroscopy. Accordingly, this study shows that high temperature rubbing of R71-P3HT at 165°C is able to enforce smectic-like order similar to that observed in RR-P3HT films rubbed at $T_R$ close to 100°C. It was therefore attempted to dope such oriented R71-P3HT films and follow the structural evolution of the films and its impact on spectroscopic and TE properties.

**2) Impact of regioregularity on the spectroscopic signatures of $F_4$TCNQ-doped P3HT**.

In a first step, we compared the impact of film doping with $F_4TCNQ$ for R71-P3HT and RR-P3HT. The evolution of the UV-vis-NIR spectra upon increasing $F_4TCNQ$ concentration is shown in Figure 2 for R71-P3HT and RR-P3HT for the orientation of light polarization parallel and perpendicular to the rubbing direction. Polarized UV-vis-NIR spectroscopy is very insightful concerning the doping mechanism of P3HT since for POL//R one probes essentially oriented and crystalline P3HT domains whereas for POL⊥R absorption stems mainly from non-oriented and disordered (amorphous) P3HT domains. Accordingly, one can probe the doping of both ordered and disordered domains by selecting the light polarization. As for RR-P3HT, doping results in the bleaching of the neutral absorption band of the polymer (N) and the emergence of polaronic P1 and P2 bands. The comparison of the position of polaronic bands in R71- and RR-P3HT indicates a substantial blue-shift of the P1 and P2 bands in rubbed more regiorandom P3HT films. In Figure 2, the maximum in absorbance for $F_4TCNQ$-doped R71-P3HT is around 2200 nm (0.58 eV) whereas for RR-P3HT it is clearly beyond 2500 nm (> 0.5 eV). Spano and coworkers demonstrated that the position of the polaronic transition is related to: i) the intrinsic polaron delocalization related to the structural order and ii) the distance between the counterion ($F_4TCNQ^{\bullet -}$) and the polaron: the larger the counterion-polaron distance, the more red-shifted is the polaron band P1.[32,33] The reduced excitonic bandwidth seen for oriented R71-P3HT suggests that planarized chain segments are shorter in the ordered R71-P3HT domains than in RR-P3HT. Accordingly, rather than a difference in polaron-counterion distance between R71-P3HT and RR-P3HT, we propose that it is the limited extent of planarized chain segments due to disorder imposed by regiorandom side chains that limits the intrinsic extension of polarons in aligned R71-P3HT films. Hence, the stronger localization of the polaron in R71-P3HT reflects the higher level of structural disorder in the aligned and ordered R71-P3HT domains as compared to RR-P3HT. The use of polarized spectroscopy gives further insight on the doping mechanism as the information

differs with the incident light polarization. For POL⊥R, the position of the P1 band in R71-P3HT films is substantially more blue-shifted to a position around 1900 nm (0.67 eV) than for POL//R. This position is consistent with reports form Lim et al. on non-oriented doped Regiorandom-P3HT (50% regioregularity).[22] The different P1 band positions in ordered and disordered R71-P3HT relates to the more localized polaron in the disordered phase of R71-P3HT i.e. red-shifted polaronic bands are expected for the more extended polarons in the ordered phase of R71-P3HT.[32,33] The comparison with oriented RR-P3HT films is telling. For RR-P3HT there is weak presence of polaronic bands in the spectra recorded for POL⊥R in $F_4$TCNQ-doped films, demonstrating marginal doping of amorphous RR-P3HT with $F_4$TCNQ. This was explained by the offset between the HOMO of amorphous RR-P3HT and the crystalline RR-P3HT that is of the order of 0.3 eV.[13] Accordingly, the disordered domains in rubbed R71-P3HT seem more readily doped than the amorphous phase of RR-P3HT. This might be a consequence of the regio-random branching of hexyl side chains in R71-P3HT. Indeed, for R71-P3HT, the $F_4$TCNQ dopant molecules may statistically access more readily close-lying sites to the polythiophene backbone than in RR-P3HT.[32,33]

Another important information given by polarized UV-vis-NIR absorption spectroscopy is related to the polarization of the $F_4TCNQ^{\bullet-}$ radical anion bands. As shown previously, in RR-P3HT, the $F_4TCNQ^{\bullet-}$ radical anion bands are polarized in a plane perpendicular to the P3HT chain direction, which is consistent with the structural model for P3HT/$F_4$TCNQ and P3HT/$F_6$TCNNQ determined by electron diffraction showing that the long axis of the dopant molecules is indeed roughly perpendicular to the P3HT backbone.[32] The same observation is made for oriented R71-P3HT films (see Figure 2). The vibronic structure of the $F_4TCNQ^{\bullet-}$ radical anion is most intense for POL//R albeit with a weaker intensity than for RR-P3HT. This indicates that the long axis of $F_4TCNQ^{\bullet-}$ molecules is

indeed on average in a plane perpendicular to the P3HT backbones of the ordered R71-P3HT domains. This is further consistent with TEM ED evidence for intercalation of dopants in the ordered domains of R71-P3HT (vide infra).

The variation of the radical anion band absorbance *versus* [$F_4$TCNQ] is also very instructive. For the films of R71-P3HT and RR-P3HT, the absorbance of the 0-0 component of the vibronic structure of the anion (at 870 nm) was measured versus [$F_4$TCNQ] (the two films have almost the same thickness). As seen in Figure S2, the amount of $F_4TCNQ^{\bullet-}$ radical anions in the R71-P3HT films saturates at a low concentration of 0.1 g/l whereas for RR-P3HT, the saturation requires a much larger concentration of [$F_4$TCNQ] (≥0.6 g/l).

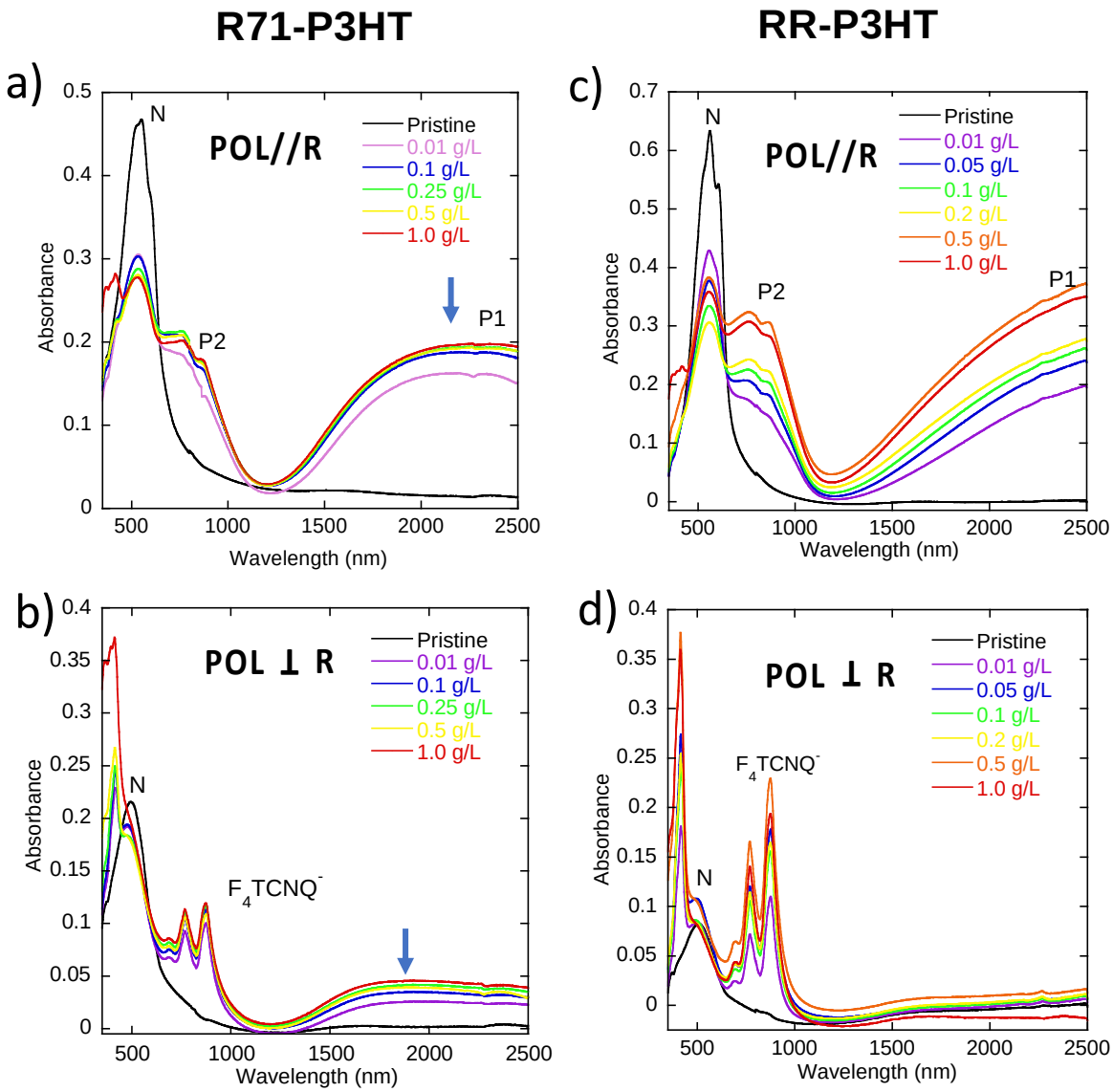

***Figure 2**. Evolution of the UV-vis-NIR spectra of aligned films of R71-P3HT ($T_R$=165°C) and RR-P3HT ($T_R$=200°C) as a function of the concentration of dopant $F_4TCNQ$ in acetonitrile. The spectra were recorded for the light polarization oriented parallel (a and c) and perpendicular (b and d) to the rubbing direction.*

The same trend is true for the polaronic band P1. The absorbances at saturation in oriented RR-P3HT for both polaron band P1 and $F_4TCNQ^{\bullet-}$ band at 870nm are about twice the ones observed for R71-P3HT. This suggests that the total amount of ionized dopants in oriented R71-P3HT films is reduced by a factor of at least 2 with respect to RR-P3HT. This is consistent with findings from Lim et al. on non-oriented R71-P3HT films reporting a 4-fold difference in the polaron intensity in regiorandom P3HT *versus* RR-P3HT.[22] The observed difference with results of Lim et al. suggests that the enhanced ordering in high-T rubbed R71-P3HT may increase slightly the doping efficiency of R71-P3HT as compared to non-oriented and highly disordered R71-P3HT films. Possibly, the fact that rubbed films show some face-on orientation is also in favor of a more effective doping since the diffusion of dopants in the layers of side chains should be eased as compared to films made of edge-on crystals.

### 2) Impact of $F_4TCNQ$-doping on the structure of aligned R71-P3HT films.

Electron diffraction in low dose is an effective method to probe the variation in lattice parameters as a function of the doping concentration. Figure 3.a and b show the typical ED patterns of oriented R71-P3HT films before and after doping with $F_4TCNQ$. In Figure 3.c and d, we show the evolution of the section profiles along the equator and the meridian for the ED patterns recorded for increasing [$F_4TCNQ$] (figure S3). The ED patterns were used to extract

the lattice parameters $d_{100}$ and $d_{020}$ that are plotted versus doping concentration in figure 3.b and 3.c for R71-P3HT and RR-P3HT, respectively.

Interestingly, the regioregularity seems to affect little the magnitude of lattice variation upon doping. R71-P3HT exhibits an evolution of the $d_{100}$ and $d_{020}$ very similar to that for RR-P3HT with a $d_{100}$ reaching 18.0±0.05 Å at 1g/l and a shortening of the π-stacking periodicity down to 3.52±0.05 Å. In particular, the lattice expansion along the side chain direction is a signature of $F_4$TCNQ intercalation in the ordered domains of RR-P3HT.[34,35] The fact that doping causes similar structural changes in R71-P3HT and RR-P3HT, suggests that the same intercalation mechanism of $F_4$TCNQ dopants in the lattice of ordered P3HT domains is at play for both polymers. This is also consistent with the polarized UV-vis-NIR results that evidenced the relative orientation of P3HT chain and long axis of dopant molecules.

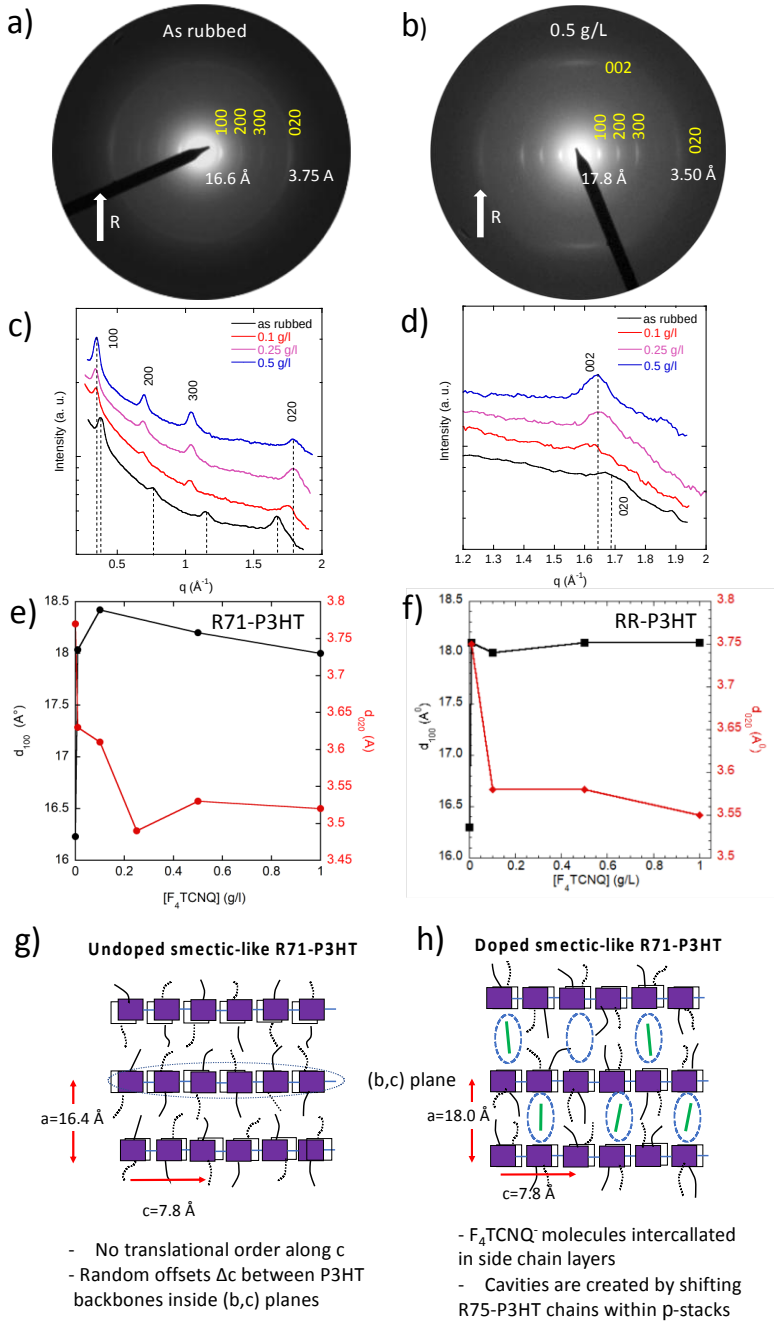


***Figure 3***. *Electron diffraction pattern of undoped (a) and doped (b) rubbed R71-P3HT thin films ($T_R$=165°C) subjected to incremental concentration doping with $F_4TCNQ$ in acetonitrile. Equatorial (c) and meridional (d) section profiles of the electron diffraction patterns of rubbed R71-P3HT films as a function of increasing [$F_4TCNQ$]. e) and f) Variation of the reticular distances $d_{100}$ (lamellar periodicity in black) and $d_{020}$ ($\pi$-stacking periodicity in red) as a function of the $F_4TCNQ$ concentration for R71-P3HT (e) and RR-P3HT (f). g) and h) Schematic illustration of the undoped (g) smectic-like structure of R71-*

*P3HT obtained by rubbing at 165°C and after doping with $F_4$TCNQ (h). The intercalation of dopant molecules inside side chain layers causes polythiophene backbones to slide within π-stack in order to group the hexyl side chains and to create the cavities (blue dotted ovals) that can host $F_4$TCNQ molecules. Both rubbing and doping promote ordering in R71-P3HT.*

Beside the lattice parameter variation, the ED patterns show an additional signature of dopant intercalation, namely the emergence of the 0 0 2 meridional reflection (Figures 3) even for very low dopant concentration of 0.1 g/l.[33] This new reflection in the doped R71-P3HT films indicates that the P3HT backbones have been shifted in the direction parallel to the chain direction to group side chains and create cavities to host $F_4$TCNQ molecules in the lattice (Figure 3.g and 3.h).[34] The doping mechanism in R71-P3HT is thus very similar to that seen for the smectic-like phase of RR-P3HT (films rubbed at 100-125°C).[13] Obviously, the initial disorder in the stacking of R71-P3HT backbones due to the regiorandom branching of the side chains does not impede the sliding of P3HT backbones in the chain direction to group the side chains and create the cavities to host the dopant molecules. This result is in line with the enhanced crystallinity seen in doped films of non-oriented RRa-P3HT.[22]

**3) Anisotropic thermoelectric properties of R71-P3HT, comparison with RR-P3HT.**

Finally, the anisotropic charge transport and thermopower were measured in the $F_4$TCNQ-doped R71-P3HT and RR-P3HT. Films doped by incremental concentration doping show an expected increase of conductivity with [$F_4$TCNQ] as seen in figure 4 with a progressive plateauing. The variation of conductivity with increasing [$F_4$TCNQ] is however substantially larger for RR-P3HT than for R71-P3HT. For R71-P3HT, the increase of σ is from 2.5 S/cm at 0.1 g/l to 3.9 S/cm at 1 g/l whereas RR-P3HT shows a more than 20-fold increase of

conductivity. It is worth to note that the maximum value of $\sigma_{//}$ obtained for R71-P3HT films rubbed at 165°C is only slightly improved *versus* that of non-oriented R71-P3HT films of the order of 1 S/cm but the value of $\sigma_{\perp}$ is close to that obtained in non-oriented films (see Figure S4). The oriented films of both polymers exhibit anisotropic charge conductivity with $\sigma_{//}/\sigma_{\perp}$ of the order of 10-11 for RR-P3HT and 5 for R71-P3HT. This is in accordance with the difference of in-plane orientation probed by UV-vis-NIR spectroscopy (see Table 1). However, there is a marked difference in the charge conductivity values at high [$F_4$TCNQ] between the two polymers. $\sigma_{//}$ saturates to a value of 4 S/cm for rubbed R71-P3HT *versus* 35 S/cm for the smectic-like phase of RR-P3HT ($T_R$=100°C) and 192 S/cm for highly aligned semi-crystalline RR-P3HT ($T_R$=200°C). The same trend is observed for $\sigma_{\perp}$. Since the apparent doping level of aligned R71-P3HT is only about ½ of that observed for rubbed RR-P3HT, the large difference in conductivity between R71- and RR-P3HT must relate for a large part to the difference in charge mobility. Although rubbing R71-P3HT films at 165°C enforces some alignment and chain planarization, it seems not sufficient to reach the conductivity observed in doped smectic-like RR-P3HT. Regioregularity defects in the chain backbone of R71-P3HT are limiting very strongly mobility in aligned R71-P3HT.[18] Accordingly, achieving order in polymer semiconductors prior to sequential doping is essential and this result is at variance with the observation of very high charge conductivity in poorly structured RR-P3HT doped electrochemically.[26] The observed difference might be related to the fact that the regime of bipolaron/polaron coexistence cannot be reached for $F_4$TCNQ-doped P3HT, due to the lower attainable level of doping.

Regarding the Seebeck coefficient, the anisotropy $\alpha_{//}/\alpha_{\perp}$ is similar for R71-P3HT and RR-P3HT at 1 g/l, typically in the range 2.2-2.5. The thermopower at 1 g/l in the direction parallel to the chains is very similar for both R71- and RR-P3HT, in the range 48-50 μV/K. However, at a lower concentration of 0.2 g/l we notice a larger anisotropy for RR-P3HT and the

thermopower is larger in the rubbing direction for RR-P3HT than for R71-P3HT. As for the conductivity, it seems that the increase of doping concentration has only limited impact on the thermopower of R71-P3HT. Turning towards the power factor, RR-P3HT reaches a value close to 50 $\mu W \cdot m^{-1} \cdot K^{-2}$ *versus* 1 $\mu W \cdot m^{-1} \cdot K^{-2}$ for R71-P3HT in the chain direction (see Figure 4). The difference in charge mobility between R71-P3HT and RR-P3HT accounts for the reduced power factor of R71-P3HT, whereas the Seebeck coefficients are quite similar for both polymers at high doping concentration, indicating that order has a more limited impact on the Seebeck coefficient than on charge conductivity. The reduced anisotropy of conductivity and thermopower in R71-P3HT are consistent with the limited alignment as well as a lower level of order evidenced by TEM ED. Overall, the present results underline the essential role of regioregularity of P3HT on TE properties and are fully in line with the previous results by Zhang et al. on the impact of regioregularity in donor-acceptor (D-A) alternated copolymers for which a 3-fold increase of the PF is observed in RR polymers.[36]

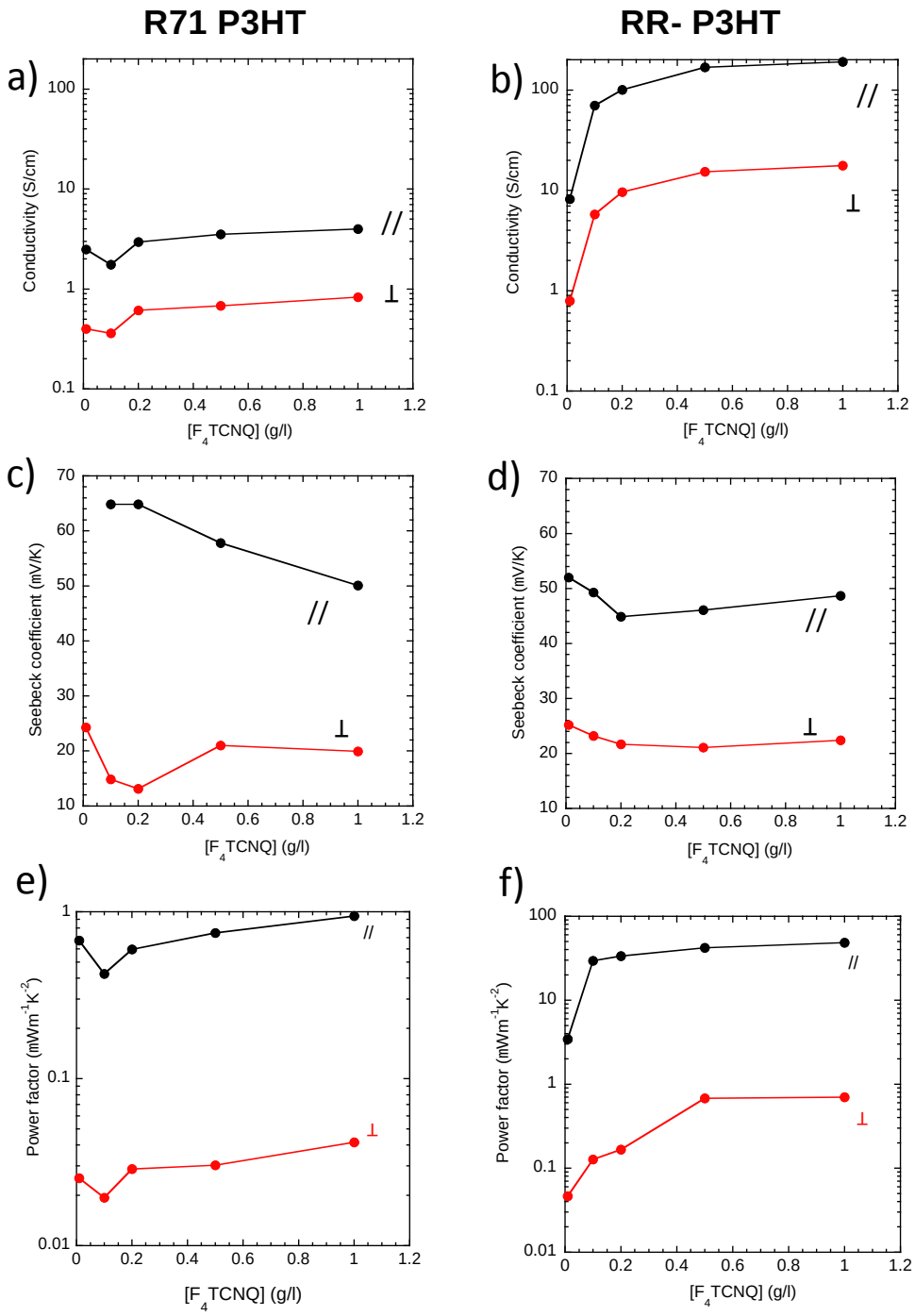


***Figure 4**. Anisotropy of the charge conductivity (a and b), of the Seebeck coefficient (c and d) and the power factor (e and f) in rubbed R71-P3HT ($T_R$=165°C) and RR-P3HT ($T_R$=200°C) measured in the direction parallel and perpendicular to the rubbing direction.*

**Table 1**. Major structural and TE characteristics of oriented and $F_4TCNQ$-doped films of RR-P3HT and R71-P3HT.

| Polymer | Optimum $T_R$ | Maximum Dichroic Ratio | Anisotropy of conductivity $\sigma_{//}/\sigma_{\perp}$ | Anisotropy of the Seebeck coefficient | Excitonic bandwith W (meV) | Maximum thermoelectric power factor ($\mu W \cdot m^{-1} \cdot K^{-2}$) |
|---|---|---|---|---|---|---|
| R71-P3HT | 165°C | 3-4 | 4.8 | 2.2 | 70±3 | 0.93±0.05 |
| RR-P3HT (60 kDa) | 200°C | 11 | 10-11 | 5 | 39±3 | 50±5 |

Further insight on TE properties can be gained from the analysis of the correlations of Seebeck coefficient and charge conductivity in the directions parallel and perpendicular to the chain direction. In the direction parallel to the polymer chains[16,25,34,37,38],

$$S_{//} \propto \sigma_{//}^{-1/4} \quad (1)$$

whereas a different behavior was observed in the direction perpendicular such that

$$S_{\perp} \propto -\log(\sigma_{\perp}) \quad (2)$$

In Figure 5, we superposed the data points obtained for R71-P3HT oriented films with the ones corresponding to RR-P3HT. As seen in Figure 5.a, the data points corresponding to R71-P3HT are down-shifted with respect to the result of the fit according to equation (1) for RR-P3HT aligned films and for different dopants. Recent studies on doped PSCs demonstrated that for non-oriented or poorly aligned films, the S-σ curves are usually down-shifted with respect to the S-σ curve for the films with high orientation.[16] The observation on S-σ data for R71-P3HT is thus fully consistent with the fact that structural order and

alignment are substantially lower in rubbed R71-P3HT as compared to RR-P3HT. In the direction perpendicular to the chains, all S-σ data points fit very well the master curve seen for RR-P3HT, indicating that TE properties of R71-P3HT are similar with the ones of the amorphous phase of RR-P3HT that is probed in the direction perpendicular to the rubbing. This result further underlines the key impact of order and orientation on S-σ correlations, as noted for doped PBTTT films.[16,34,37]

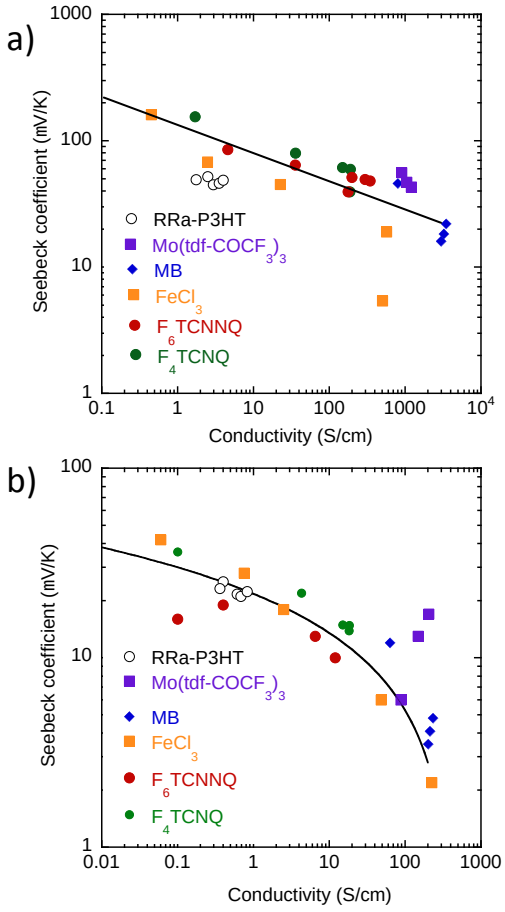


**Figure 5**. Correlations between Seebeck coefficient and charge conductivity measured in the directions parallel (a) and perpendicular (b) to the chain direction (rubbing direction) for RR-P3HT thin films doped with various dopants as well as for oriented R71-P3HT doped with $F_4TCNQ$.

## III. Conclusion.

High temperature rubbing is able to induce order and alignment in thin films of R71-P3HT that is comparable to that found for the smectic-like phase of RR-P3HT when rubbed at 100°C. Incremental concentration doping further improves order and promotes crystallization of R71-P3HT. The doping mechanism bears similarities with that of RR-P3HT. Intercalation of $F_4TCNQ$ dopant molecules occurs in the ordered R71-P3HT domains causing: i) a reorganization of the poly(thiophene) backbones within π-stacks similar to that evidenced for the smectic-like phase of RR-P3HT, ii) a contraction of π-stacking periodicity and iii) expansion of the lattice in the side-chain direction. The thermoelectric performances of oriented-R71-P3HT approach those of non-oriented RR-P3HT, but the obtained charge conductivities in the chain direction are 5-times below that of the aligned smectic phase of RR-P3HT ($T_R$=100°C) and almost 50-times below that of oriented semi-crystalline RR-P3HT ($T_R$=200°C). This reduced charge transport is due to i) a reduced doping level in R71-P3HT (by a factor of approximately ½) and ii) to a reduced charge mobility because of the stronger localization of the charge carriers as suggested by Polarized UV-vis-NIR spectroscopy. Overall, this work demonstrates that the initial level of order in the undoped pristine P3HT films that is determined by regioregularity is essential to achieve high TE performances. It will be important to further investigate if by using stronger dopants such as magic blue ($FeCl_3$) that can dope amorphous (amorphous and crystalline) zones, it could be possible to further increase the conductivity in oriented R71-P3HT and approach the values reported for electrochemically doped P3HT.

## Supporting information.

Electron diffraction pattern as a function of the rubbing temperature $T_R$ , Evolution of the absorbance of the vibronic structure of $F_4TCNQ^-$ anion as a function of [$F_4TCNQ$] for oriented R71-P3HT and RR-P3HT films. Evolution of the absorbance of the polaron band P1 for R71-P3HT and RR-P3HT as a function of [$F_4TCNQ$]. Correlation of the absorbances of the P1 band and of the $F_4TCNQ^-$ anion for R71-P3HT and RR-P3HT. Evolution of the ED pattern of rubbed P3HT-R75 aligned at $T_R$=165°C upon doping with $F_4TCNQ$. Evolution of the charge conductivity, the Seebeck coefficient and the thermoelectric power factor for non-oriented R71-P3HT thin films. $^1$H-NMR spectrum of R71-P3HT

**Acknowledgments.**

Bernard Lotz is gratefully acknowledged for fruitful discussions and careful reading of the manuscript. C. Blanck and M. Schmutz are acknowledged for technical support in TEM. N. Zimmermann is acknowledged for technical support in pre-patterned device preparation. O. Boyron is acknowledged for the SEC measurement. Financial support from ANR grant Anisotherm ANR-17-CE05-0012 (ANISOTHERM) is acknowledged. This work was financially supported by the European Commission through Marie Sklodowska-Curie project HORATES (GA-955837).

**Conflict of interest.**

The authors declare no conflict of interest.

**IV. Experimental section.**

Regio-regular P3HT was purchased from Ossila ($M_w$ = 60.15 kDa, $M_n$=28.65 kDa and D=2.1, RR=97.6%). $F_4TCNQ$ was purchased from TCI. Anhydrous solvents (99%) used for doping (acetonitrile) and film preparation (ortho-dichlorobenzene) as well as sodium poly(styrenesulfonate) (NaPSS) and dichloromethane were purchased from Sigma Aldrich. Hexyl thiophene was purchased from TCI, Tokyo Chemical Industry ( >98,0%) . Iron

chloride was purchased from Merck (≥98,0%) and LiTFSI was bought from Solvionic (<20 ppm $H_2O$, >99,9%).

Regio-random P3HT (R71-P3HT) ($M_n$= 30.9 kDa and $M_w$=96.4 kDa, D=3.1) was synthesized by heterogeneous oxidative chemical polymerization by introducing dropwise under stirring 10 mL of a solution of the monomer 3HT (1.5g, 8.91 mmol in dichloromethane-) into a 100 mL single flask containing 30 mL of a suspension of 2.33 equivalents of $FeCl_3$ in $CH_2Cl_2$. (3.37g, 20.8 mmol). After 24h of stirring at ambient temperature, the black viscous reactant liquid is extracted on filter paper and washed with distilled ethanol until colorless liquid is observed, a sign that the excess of iron trichloride is eliminated. Finally, the RRa P3HT is de-doped with 100 mL of a 5% aqueous ammonia solution (Fisher chemical). The black solid is dried 24h under vacuum at 45°C. A yield of 80% was obtained. The ratio of head to tail (HT) and head to head (HH) arrangement of repeat units in polymer chain can be determined from characteristic α-methylene peaks.[39,40] The peak in the range of 2.75 to 2.8 ppm is attributed to HT arrangement whereas the peak in the range of 2.5 to 2.6 ppm is due to HH arrangement. The percentage of HH and HT content can be estimated from the relative ratio of the integral of above-mentioned peaks. P3HT $^1$H NMR spectrum was recorded in deuterated $CDCl_3$ on a Bruker Avance III HD – 500 MHz. In our case, this measurement gave a regioregularity of about 71 ± 3% (see Figure S5). The measurements of molecular weight were carried out using a Malvern Panalytical size exclusion chromatography (SEC). THF was used as the mobile phase at a flow rate of 1 mL min$^{-1}$ at 40 °C. The samples were injected at a concentration of around 4 mg mL-1 after filtration on a 0.45 µm PTFE membrane. The separation was achieved on three Agilent mixed C columns (SDVB, 5 µm, 300 x 7.5 mm). Molecular weights were calculated using a conventional calibration curve based on certified PS standards (Polymer Standards Service) from 470 to 2,500,000 g mol-1. Omnisec 5.12 software (Malvern Panalytical) was used to acquire and process the data.

The orientation of the R71-P3HT and RR-P3HT films followed the protocol described in previous publications using the method of high-T rubbing.[26,13] A homemade set-up is used, it consists of a rotating cylinder covered with a microfiber cloth and a translating hot plate. The film thickness was extracted from the UV-vis absorbance using the calibration given in reference 23. P3HT films were deposited by doctor blading from a 15g/l solution in ODCB at 154°C on glass substrates covered with a sacrificial layer of NaPSS. NaPSS was spincoated at 3000 RPM from 10g/l acqueous solution on glass substrates cleaned by ultrasonication in acetone, ethanol, hellmanex and deionized water (x3 times).

The doping of P3HT films with $F_4TCNQ$ was performed following the incremental concentration doping (ICD) procedure with full sample immersion for 1 min in the dopant solution in acetonitrile of increasing concentration.[40] No rinsing of the doped P3HT films was performed after doping as it causes unwanted dedoping. Doping was performed in a Jacomex glovebox under inert atmosphere.

**b) Structural analysis by TEM.** Oriented P3HT films were coated with a thin amorphous carbon film (Edwards Auto306 evaporator). The films were floated on distilled water and recovered on TEM copper grids. A CM12 Philips microscope (120 kV) equipped with a MVIII (Soft Imaging System) charge coupled device camera TEM was used for bright field and electron diffraction (ED) analysis. Oriented poly(tetrafluoroethylene) substrate was used as a reference to calibrate the ED patterns. Beam exposure was minimized (low dose system) to avoid de-doping of the oriented films under the electron beam. AFM was performed with a Multimode 8 Bruker with Nanoscope V controller using ScanAsyst-Air tips (0.4N/m).

**c) Polarized UV–Vis–NIR absorption**. A Varian Cary 5000 spectrometer with polarized incident light (spectral resolution of 1 nm) was used to probe the film orientation and the

effect of doping with $F_4TCNQ$ as a function of doping concentration. The angle of light polarization is measured with respect to the rubbing direction (0° corresponding to the light polarization POL//R and 90° corresponding to the light polarization POL⊥R).

**d) Charge conductivity and Seebeck coefficient.** Cleaned glass substrates were dried under nitrogen and exposed to plasma prior to electrode deposition. Gold electrical contacts (40 nm thick) in a four-points probe geometry (1 mm spacing between electrodes, 5 mm length) were deposited via high vacuum thermal evaporation through a shadow mask ( rate of 4–6 Å/s). The geometry of the electrodes allows to measure anisotropic charge transport and thermopower on a same substrate in both parallel and perpendicular directions to the rubbing. Oriented films of P3HT were floated on water and carefully recovered on the device with pre-deposited gold electrodes. They were subsequently doped using the ICD protocol.[37,40]

All measurements of DC conductivity and Seebeck coefficients were performed in a Jacomex glovebox under $N_2$ atmosphere (< 1 ppm $H_20$ and < 2 ppm $O_2$). Four-point probe measurements of electrical conductivity were performed using a Keithley 2634B and a Lab Assistant Semiprobe station. The resistivity ρ was derived from the sheet resistance R following the relation $\rho = 1.81 \cdot R \cdot t$ where t is the film thickness (the geometrical correction factor was determined following the method in reference 15. The film thickness was determined from the UV-vis absorbance using the calibration provided in references 24 for P3HT.

The thermopower was measured using a differential temperature method whereby a temperature gradient was established across the sample along or perpendicular to the rubbing direction. The temperature gradient was ramped between 0 and 12K around room temperature and the Seebeck coefficient was extracted by plotting the thermovoltage versus temperature gradient. A constantan wire was used to calibrate the Seebeck coefficient. The detailed procedure is given in reference 15.

**References.**


(1) Goel, M.; Thelakkat, M. Polymer Thermoelectrics: Opportunities and Challenges. *Macromolecules* **2020**, *53* (10), 3632–3642.

(2) review TE systems

(3) R. Kroon, D. A. Mengistie, D. Kiefer, J. Hynynen, J. D. Ryan, L. Yu and C. Müller, *Chem. Soc. Rev.*, 2016, **45**, 6147–6164.

(4) A. D. Scaccabarozzi, A. Basu, F. Aniés, J. Liu, O. Zapata-Arteaga, R. Warren, Y. Firdaus, M. I. Nugraha, Y. Lin, M. Campoy-Quiles, N. Koch, C. Müller, L. Tsetseris, M. Heeney and T. D. Anthopoulos, *Chem. Rev.*, 2022, **122**, 4420–4492.

(5) Jacobs, I. E.; Moulé, A. J. Controlling Molecular Doping in Organic Semiconductors. *Advanced Materials* **2017**, *29* (42), 1703063.

(6) Zhao, W.; Ding, J.; Zou, Y.; Di, C.; Zhu, D. Chemical Doping of Organic Semiconductors for Thermoelectric Applications. *Chem. Soc. Rev.* **2020**, *49* (20), 7210–7228. https://doi.org/10.1039/D0CS00204F.

(7) Scholes, D. T.; Hawks, S. A.; Yee, P. Y.; Wu, H.; Lindemuth, J. R.; Tolbert, S. H.; Schwartz, B. J., Overcoming Film Quality Issues for Conjugated Polymers Doped with F4TCNQ by Solution Sequential Processing: Hall Effect, Structural, and Optical Measurements. *J. Phys. Chem. Lett.* **2015**, 6, 4786–4793.

(8) Scholes, D. T.; Yee, P. Y.; Lindemuth, J.R.; Kang, H.; Onorato, J.; Ghosh, R.; Luscombe, C. K.; Spano, F. C.; Tolbert, S. H.; Schwartz, B. J., The Effects of Crystallinity on Charge Transport and the Structure of Sequentially Processed F4TCNQ-Doped Conjugated Polymer Films. *Adv. Funct. Mater.***2017**, 27, 1702654.

(9) Duong, D. T.; Wang, C.; Antono, E.; Toney, M. F.; Salleo, A. The Chemical and Structural Origin of Efficient P-Type Doping in P3HT. *Organic Electronics* **2013**, *14* (5), 1330–1336.

(10) Glaudell, A. M.; Cochran, J. E.; Patel, S. N.; Chabinyc, M. L. Impact of the Doping Method on Conductivity and Thermopower in Semiconducting Polythiophenes. *Advanced Energy Materials* **2015**, *5* (4), 1401072.

(11) Patel, S. N.; Glaudell, A. M.; Peterson, K. A.; Thomas, E. M.; O'Hara, K. A.; Lim, E.; Chabinyc, M. L. Morphology Controls the Thermoelectric Power Factor of a Doped Semiconducting Polymer. *Science Advances* **2017**, *3*, e1700434

(12) Hynynen, J.; Kiefer, D.; Yu, L.; Kroon, R.; Munir, R.; Amassian, A.; Kemerink, M.; Müller, C. Enhanced Electrical Conductivity of Molecularly P-Doped Poly(3-Hexylthiophene) through Understanding the Correlation with Solid-State Order. *Macromolecules* **2017**, *50* (20), 8140–8148. https://doi.org/10.1021/acs.macromol.7b00968.

(13) Untilova, V.; Biskup, T.; Biniek, L.; Vijayakumar, V.; Brinkmann, M. Control of Chain Alignment and Crystallization Helps Enhance Charge Conductivities and Thermoelectric Power Factors in Sequentially Doped P3HT:F4TCNQ Films. *Macromolecules* **2020**, *53*, 2441.

(14) Patel, S. N.; Chabinyc, M. L. Anisotropies and the Thermoelectric Properties of Semiconducting Polymers. *Journal of Applied Polymer Science* **2017**, *134* (3), 44403

(15) Hamidi-Sakr, A.; Biniek, L.; Bantignies, J.-L.; Maurin, D.; Herrmann, L.; Leclerc, N.; Lévêque, P.; Vijayakumar, V.; Zimmermann, N.; Brinkmann, M. A Versatile Method to Fabricate Highly In-Plane Aligned Conducting Polymer Films with Anisotropic Charge Transport and Thermoelectric Properties: The Key Role of Alkyl Side Chain Layers on the Doping Mechanism. *Advanced Functional Materials* **2017**, 27, 1700173.

(16) Degousée, T.; Untilova, V.; Vijayakumar, V.; Xu, X.; Sun, Y.; Palma, M.; Brinkmann, M.; Biniek, L.; Fenwick, O. High Thermal Conductivity States and Enhanced Figure of Merit in Aligned Polymer Thermoelectric Materials. *J. Mater. Chem. A* **2021**, *9* (29), 16065–16075. https://doi.org/10.1039/D1TA03377H.

(17) Durand, P.; Zeng, H.; Biskup, T.; Vijayakumar, V.; Untilova, V.; Kiefer, C.; Heinrich, B.; Herrmann, L.; Brinkmann, M.; Leclerc, N. Single Ether-Based Side Chains in Conjugated Polymers: Toward Power Factors of 2.9 MW M−1 K−2. *Advanced Energy Materials* **2022**, *12* (2), 2103049. https://doi.org/10.1002/aenm.202103049.

(18) Zeng, H.; Durand, P.; Guchait, S.; Herrmann, L.; Kiefer, C.; Leclerc, N.; Brinkmann, M. Optimizing Chain Alignment and Preserving the Pristine Structure of Single-Ether Based PBTTT Helps Improve Thermoelectric Properties in Sequentially Doped Thin Films. *J. Mater. Chem. C* **2022**, *10* (42), 15883–15896. https://doi.org/10.1039/D2TC03600B.

(19) Poelking, C.; Andrienko, D. Effect of Polymorphism, Regioregularity and Paracrystallinity on Charge Transport in Poly(3-Hexylthiophene) [P3HT] Nanofibers. *Macromolecules* **2013**, *46* (22), 8941–8956. https://doi.org/10.1021/ma4015966.

(20) Kim, J.-S.; Kim, J.-H.; Lee, W.; Yu, H.; Kim, H. J.; Song, I.; Shin, M.; Oh, J. H.; Jeong, U.; Kim, T.-S.; Kim, B. J. Tuning Mechanical and Optoelectrical Properties of Poly(3-Hexylthiophene) through Systematic Regioregularity Control. *Macromolecules* **2015**, *48* (13), 4339–4346. https://doi.org/10.1021/acs.macromol.5b00524.

(21) Kim, Y.; Park, H.; Park, J. S.; Lee, J.-W.; Kim, F. S.; Kim, H. J.; Kim, B. J. Regioregularity-Control of Conjugated Polymers: From Synthesis and Properties, to Photovoltaic Device Applications. *J. Mater. Chem. A* **2022**, *10* (6), 2672–2696. https://doi.org/10.1039/D1TA08495J.

(22) Lim, E.; Glaudell, A. M.; Miller, R.; Chabinyc, M. L. The Role of Ordering on the Thermoelectric Properties of Blends of Regioregular and Regiorandom Poly(3-Hexylthiophene). *Advanced Electronic Materials* **2019**, *5* (11), 1800915. https://doi.org/10.1002/aelm.201800915.

(23) Yee, P. Y.; Scholes, D. T.; Schwartz, B. J.; Tolbert, S. H. Dopant-Induced Ordering of Amorphous Regions in Regiorandom P3HT. *J. Phys. Chem. Lett.* **2019**, *10* (17), 4929–4934. https://doi.org/10.1021/acs.jpclett.9b02070.

(24) Untilova, V.; Hynynen, J.; Hofmann, A. I.; Scheunemann, D.; Zhang, Y.; Barlow, S.; Kemerink, M.; Marder, S. R.; Biniek, L.; Müller, C.; Brinkmann, M. High Thermoelectric Power Factor of Poly(3-Hexylthiophene) through In-Plane Alignment and Doping with a Molybdenum Dithiolene Complex. *Macromolecules* **2020**, *53* (15), 6314–6321. https://doi.org/10.1021/acs.macromol.0c01223.

(25) Zhong, Y.; Untilova, V.; Muller, D.; Guchait, S.; Kiefer, C.; Herrmann, L.; Zimmermann, N.; Brosset, M.; Heiser, T.; Brinkmann, M. Preferential Location of Dopants in the Amorphous Phase of Oriented Regioregular Poly(3-Hexylthiophene-2,5-Diyl) Films Helps Reach Charge Conductivities of 3000 S Cm−1. *Advanced Functional Materials* **2022**, *32* (30), 2202075. https://doi.org/10.1002/adfm.202202075.

(26) Neusser, D.; Malacrida, C.; Kern, M.; Gross, Y. M.; van Slageren, J.; Ludwigs, S. High Conductivities of Disordered P3HT Films by an Electrochemical Doping Strategy. *Chem. Mater.* **2020**, *32* (14), 6003–6013. https://doi.org/10.1021/acs.chemmater.0c01293.

(27) Hamidi-Sakr, A.; Biniek, L.; Fall, S.; Brinkmann, M., Precise Control of Lamellar Thickness in Highly Oriented Regioregular Poly(3-Hexylthiophene) Thin

Films Prepared by High-Temperature Rubbing: Correlations with Optical Properties and Charge Transport. *Adv. Funct. Mater.* **2016**, 26, 408–420.

(28) Hartmann, L.; Tremel, K.; Uttiya, S.; Crossland, E.; Ludwigs, S.; Kayunkid, N.; Vergnat, C.; Brinkmann, M. 2D Versus 3D Crystalline Order in Thin Films of Regioregular Poly(3-Hexylthiophene) Oriented by Mechanical Rubbing and Epitaxy. *Advanced Functional Materials* **2011**, *21* (21), 4047–4057. https://doi.org/10.1002/adfm.201101139.

(29) Clark, J.; Chang, J.-F.; Spano, F. C.; Friend, R. H.; Silva, C., Determining exciton bandwidth and film microstructure in polythiophene films using linear absorption spectroscopy. *Appl. Phys. Lett.* **2009**, 94, 163306.

(30) Spano, F. C. Modeling disorder in polymer aggregates: The optical spectroscopy of regioregular poly(3-hexylthiophene) thin films. *J. Chem. Phys.* **2005**, 122, 234701.

(31) The ratio of the absorbances of the 0-0 and 0-1 contributions to the vibronic structure of the absorption spectra are given by the equation : $A_{0\text{-}0}/A_{0\text{-}1}=[(1\text{-}0.24W/E_p)/(1+0.073W/E_p)]^2$ where W is the excitonic bandwidth and $E_p$ the energy of the intra-molecular vibrational energy taken as $E_p$=0.18 eV.

(32) Ghosh, R.; Pochas, C. M.; Spano, F. C. Polaron Delocalization in Conjugated Polymer Films. *J. Phys. Chem. C* **2016**, *120* (21), 11394–11406. https://doi.org/10.1021/acs.jpcc.6b02917.

(33) Scholes, D. T.; Yee, P. Y.; Lindemuth, J.R.; Kang, H.; Onorato, J.; Ghosh, R.; Luscombe, C. K.; Spano, F. C.; Tolbert, S. H.; Schwartz, B. J., The Effects of Crystallinity on Charge Transport and the Structure of Sequentially Processed F4TCNQ-Doped Conjugated Polymer Films. *Adv. Funct. Mater.***2017**, 27, 1702654.

(34) Untilova, V.; Zeng, H.; Durand, P.; Herrmann, L.; Leclerc, N.; Brinkmann, M. Intercalation and Ordering of F6TCNNQ and F4TCNQ Dopants in Regioregular Poly(3-Hexylthiophene) Crystals: Impact on Anisotropic Thermoelectric Properties of Oriented Thin Films. *Macromolecules* **2021**, *54* (13), 6073–6084. https://doi.org/10.1021/acs.macromol.1c00554.

(35) Comin, M.; Lemaur, V.; Giunchi, A.; Beljonne, D.; Blase, X.; D'Avino, G. Doping of Semicrystalline Conjugated Polymers: Dopants within Alkyl Chains Do It Better. *J. Mater. Chem. C* **2022**, *10* (37), 13815–13825. https://doi.org/10.1039/D2TC01115H.

(36) Zhang, Y.; Deng, L.; Cho, Y.; Lee, J.; Shibayama, N.; Zhang, Z.; Wang, C.; Hu, Z.; Wang, J.; Wu, F.; Chen, L.; Du, Y.; Ren, F.; Yang, C.; Gao, P. Revealing the Enhanced Thermoelectric Properties of Controllably Doped Donor-Acceptor

Copolymer: The Impact of Regioregularity. *Small* **2023**, *n/a* (n/a), 2206233. https://doi.org/10.1002/smll.202206233.

(37) Vijayakumar, V.; Zhong, Y.; Untilova, V.; Bahri, M.; Herrmann, L.; Biniek, L., Leclerc N.; Brinkmann, M., Bringing conducting polymers to high order: towards conductivities beyond $10^5$ S/cm and thermoelectric power factors of 2 $mW \cdot m^{-1} \cdot K^{-2}$. *Adv. En. Mater.* **2019**, 1900266.

(38) Scheunemann, D.; Vijayakumar, V.; Zeng, H.; Durand, P.; Leclerc, N.; Brinkmann, M.; Kemerink, M. Rubbing and Drawing: Generic Ways to Improve the Thermoelectric Power Factor of Organic Semiconductors? *Advanced Electronic Materials* **2020**, *6* (8), 2000218. https://doi.org/10.1002/aelm.202000218.

(39) Trznadel, M.; Pron, A.; Zagorska, M.; Chrzaszcz, R.; Pielichowski, J. Effect of Molecular Weight on Spectroscopic and Spectroelectrochemical Properties of Regioregular Poly(3-Hexylthiophene). *Macromolecules* **1998**, *31* (15), 5051–5058. https://doi.org/10.1021/ma970627a.

(40) Ansari, M. A.; Mohiuddin, S.; Kandemirli, F.; Malik, M. I. Synthesis and Characterization of Poly(3-Hexylthiophene): Improvement of Regioregularity and Energy Band Gap. *RSC Adv.* **2018**, *8* (15), 8319–8328. https://doi.org/10.1039/C8RA00555A.

(41) Vijayakumar, V.; Durand, P.; Zeng, H.; Untilova, V.; Herrmann, L.; Algayer, P.; Leclerc, N.; Brinkmann, M. Influence of Dopant Size and Doping Method on the Structure and Thermoelectric Properties of PBTTT Films Doped with F6TCNNQ and F4TCNQ. *J. Mater. Chem. C* **2020**, *8* (46), 16470–16482. https://doi.org/10.1039/D0TC02828B.

*For Table of Contents Only*